

<https://doi.org/10.70917/ijcisim-2026-0032>  
Article

# Research on Cultural Characteristics and Environmental Adaptability in Public Space Using Artificial Intelligence-Assisted Design

Weiwei Hou \*

School of Design, Xuzhou University of Technology, Xuzhou, Jiangsu, 221000, China; pnl8058@163.com

**Abstract:** As the main activity place to meet the public needs of residents in the city, the overall design of public space presents cultural characteristics and environmental integration, which is closely related to the satisfaction of the residents and the appearance of the city. This paper proposes a collaborative filtering-based public space layout algorithm by combining the distribution probability of design features and user interest characteristics. The deep neural network is used to extract the features of different spatial functional requirements and spatial layout parameters from the distribution structure and distribution pattern of the layout space. After obtaining the overall layout scheme and layout parameter features, the optimal layout scheme is determined by minimizing the energy function in the layout method. The graph-driven MH layout optimization (GD-MH) algorithm is improved to optimize the spatial layout, and a public space layout design method based on the GA-MH algorithm is formed comprehensively. The designed method is able to optimize the layout scheme with an interference of 0mm compared with similar methods.

**Keywords:** public space layout design; GA-MH algorithm; deep neural network; energy function

## 1. Introduction

Since the beginning of the industrial revolution, the rapid progress of technology level promotes the development of various production and construction activities, and leads to the rapid evolution of urbanization. However, industrialization in driving the rapid development of the city at the same time, inevitably caused a certain impact on the regional culture, part of the quick success and short-term profit, the lack of humanities in the construction mode, so that the homogenization tendency is getting more and more intense [1]. For urban public space, “top-down” human intervention makes the spatial form of public space present regularized order, and its original cultural characteristics and environmental adaptability has been damaged, which leads to the public space of the “culture, originality” constantly alienation [2-4]. The disorder of urban pattern, the loss of public space culture, the loss of historical places and many other destructive problems come one after another [5]. In the face of the rapid development of modernization and the problems and challenges brought to urban public space, it is urgent to explore a beneficial path focusing on the revitalization and protection of urban public space, to pass on its core values, so as to be able to retain its cultural characteristics, to perfect its unique material space form, social and cultural form, and to realize the enhancement of the cultural identity of the aborigines [6].

However, traditional public space design methods are limited by subjective consciousness and designers' experience, and are unable to fully consider various complex factors and constraints [7]. However, with the rapid development of AI technology, AI-based assisted design methods are becoming an innovative solution [8]. Assisted design methods based on AI technology utilize techniques such as big data analysis, machine learning, and optimization algorithms to perform layout optimization and spatial planning in a data-driven manner [9-11]. By collecting and analyzing data, behavioral patterns and preferences, as well as predicting market trends, design teams are able to generate personalized design solutions that are optimized and adjusted by automated layout generation algorithms and space



optimization algorithms [12]. This emerging design methodology not only enhances design efficiency but also delivers public-space solutions that are culturally distinctive and environmentally adaptable.

The emergence of artificial intelligence-assisted design tools has provided new ideas for designers' idea generation efforts. Guridi, J. A et al. [13] argued that Image Generating Artificial Intelligence (IGAI) transforms the collaborative design process of public spaces, and its ability to increase the diversity, engagement, and efficiency of the design of public spaces by strengthening the ability to translate the public's needs into visual features. Li, H et al. [14] investigated the integration of artificial intelligence and architectural spatial intelligence with the aim of improving designers' design efficiency and innovation in public space, and the results showed that AI-assisted design methods are superior to traditional methods and have practical application value in the digital transformation of spatial design. Chen, T. Y et al [15] used artificial intelligence-driven simulation to optimize the design of an urban park by implementing design improvements such as shading facilities and vegetation layout to enhance the comfort of the public space, and the resulting design solution demonstrated long-term sustainability and environmental adaptability. Quan, S. J et al. [16] integrated elements of AI-assisted design, design thinking, simulation, and participation to construct an intelligent design framework, which aims to address the limitations of current urban public space planning systems. In summary, the importance of AI-assisted design for urban public space design should not be ignored, which can not only provide a better public space experience and comfort, but also improve the functionality, safety, and sustainability of public space.

This paper firstly explains the construction process of public space layout algorithm based on multi-person collaboration. It also chooses information entropy as the structural feature of spatial distribution of the main functional area, and explains the extraction method and steps of the spatial distribution feature of the main functional area of public space under the deep neural network. Then the process of minimizing the energy function to determine the best layout scheme and the optimization of the MH algorithm are described, and the layout scheme generation method based on the GD-MH algorithm is proposed, which in turn establishes the public space layout design method based on the GD-MH algorithm. Subsequently, the variation operator is determined, and the convergence effect of the proposed GD-MHG algorithm and similar algorithms is compared. Finally, suitable arithmetic examples are selected to compare the overall layout design effect of similar algorithms with the algorithm in this paper.

## **2. Public Space Layout Design Based on GD-MH Algorithm**

### *2.1. Design of Public Space Layout Algorithms Based on Multiplayer Collaboration*

After the public space layout feature extraction based on collaborative filtering is finished, the frequency of design content feature word distribution and user interest features are obtained, and then the public space layout weight design is adopted to design the public space layout algorithm with multiple collaborators. Firstly, the weight of public space layout and the user's rating result of the design are calculated, and the overall layout design time is effectively shortened in this way. Second, according to the distribution of feature words, the public space layout design document set is constructed, and based on the content of the document set, the linear design matrix structure of the optimized house is obtained, and the corresponding layout design optimization function is obtained. Finally, based on the multi-person collaborative design algorithm to predict the scoring results of the house building design, to help the designer to carry out the overall design of the public space layout. The flow structure of the public space layout algorithm based on multiplayer collaboration constructed in this paper is shown in Figure 1.

The steps of the public space layout algorithm based on multiplayer collaboration are as follows: first, filter the space layout dataset by multiplayer collaborative algorithm to obtain the number of layout items  $N$ . Second, the collaborative filtering algorithm is used to calculate the public space distribution weights, count the number of occurrences of user feature words, and determine the types of spatial layout designs with higher user interest. Third, the weight matrix is constructed based on the results of the public space distribution weights, and the dimensionality of the matrix is considered comprehensively during the construction. Fourth, according to the predicted public space distribution results, calculate the cost function by utilizing multi-person collaboration. Fifth, update the relevant parameters in the cost function in a timely manner to ensure stable changes in the cost function and reduce the gradient of the spatial distribution design. Sixth, adjust the average deviation of the public space layout design to provide users with a public space layout design scheme with high adaptability.

The public space layout algorithm for designing multi-person collaboration can cover the entire layout definition domain, divide all the housing buildings into the layout definition domain, and ensure the balance of the relative positional relationship of the definition domain.

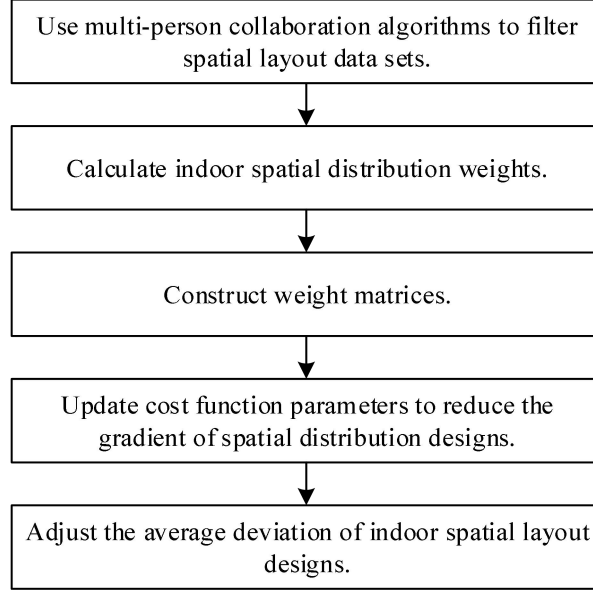


**Figure 1.** Public space layout algorithm based on multi-person collaboration.

## 2.2. Extracting the Spatial Distribution Characteristics of the Main Functional Areas of Public Space

Before optimizing the layout of the main functional area of public space, the layout space distribution characteristics are extracted based on the collected and processed functional area spatial data. In this paper, we mainly obtain the distribution structure and distribution pattern of the layout space from two aspects. Due to the more complex nature of the land use of the main functional area of public space, the information entropy is selected as the spatial distribution structure feature of the main functional area, and the information entropy value of the spatial feature is equation (1):

$$\delta = -\sum \left( \frac{S_n}{S_0} \right) \ln \left( \frac{S_n}{S_0} \right) \quad (1)$$

where:  $S_0$  is the total area of each functional area.  $S_n$  is the area of the  $n$ th functional area. In general, when the information entropy obtained from equation (1) is 0, it indicates that the functional area is not developed. On the contrary, if the information entropy is the maximum value, it indicates that the development of the functional area has stabilized. Therefore, when optimizing the layout of the main functional area of public space, it is necessary to combine the information entropy to determine the development of land in various functional areas. In this paper, in order to determine the degree of disposability of land types in the main functional area of public space, the degree of equilibrium is chosen as the second feature of spatial structure. The expression of equilibrium degree of land in each functional area of public space is equation (2):

$$\eta = \frac{\delta}{\ln(N)} \quad (2)$$

where:  $N$  is the number of types of land in each functional area of public space. Usually the equilibrium degree of the formula (2) is  $[0, 1]$ , if the equilibrium degree is 0, it indicates that the land in the functional area is in an unbalanced state of use. On the contrary, if the required degree of equilibrium is 1, it indicates that the land use of the functional area has reached the ideal state of equilibrium.

In this paper, shape rate and compactness are taken as the spatial distribution characteristics of the main functional area of public space. The shape rate feature can measure the number of shapes in the functional area. The expression of shape rate of each functional area is equation (3):

$$\lambda = \frac{S_1}{L^2} \quad (3)$$

where:  $S_1$  is the area of the region.  $L$  is the length of the region. If the value of the shape rate obtained from equation (3) is small, it indicates that the region is more distinctive in terms of banding characteristics. On the contrary, if the value of shape rate is larger, it indicates that the region is block-like distribution.

Compactness is mainly used to measure the shape characteristics of the functional area region. The expression for the compactness of the layout of each functional area region is equation (4):

$$\mu = \frac{S_1}{S_1} \quad (4)$$

where:  $S_1$  is the minimum outer circle area of the functional area. Deep neural network is utilized to extract the spatial distribution characteristics of the main functional area of public space.

The deep neural network is used to collect the relevant feature points, calculate the corresponding measurement function index parameters, and determine whether it is suitable for carrying out layout optimization design. The formula for calculating the characteristic index parameters is equation (5):

$$A = b + \frac{w}{r(s-w)} \quad (5)$$

where:  $b$  is the upper limit of eigenvalue.  $r$  is the optimization coefficient of characteristic parameters.  $s$  is the distribution range.  $w$  is the lower limit of eigenvalue. After the operation, the corresponding eigenvalue index parameters are determined. Using the calculated feature index parameters, the layout feature extraction results of the functional area are evaluated, and once the value range is exceeded, it indicates that there are abnormalities in the feature extraction, and it is necessary to re-extract them, otherwise, it indicates that the layout feature extraction results are suitable for the layout optimization design, and the subsequent operations can be carried out.

### 2.3. Layout Scheme Generation Based on GD-MH Algorithm

#### 2.3.1. Energy Function

After the existence of the layout information in the hierarchical graph structure (SG), it is necessary to create an effective layout as in equation (6):

$$SG^* = \arg \min_S \sum_{V_i \in V} E_r(S) \quad (6)$$

where  $E_r$  is the weighted sum of the following energy terms, and the optimal layout plan is determined by minimizing this energy function.

(1) Space requirement. There needs to be open space around the objects in the group. Spacing also needs to be maintained between groups and between groups and walls as walking paths. Equation (7) shows the energy function for the space constraint  $E_s$ .

$$E_s = \sum \varphi(\varepsilon - 2\varepsilon\sigma(\alpha(S_i) + \alpha(M_i) + \alpha(W_i))) \quad (7)$$

where:  $\alpha(S_i)$  is the area of spatial overlap between objects in the group.  $\alpha(M_i)$  is the area of overlap between groups.  $\alpha(W_i)$  is the area of spatial overlap between walls and groups.  $\beta(S)$  is the total space requirement area.  $\varepsilon$  is a constant taken as 1.5.  $\sigma(x)$  is the sigmoid function.  $\varphi(x)$  is expressed as equation (8):

$$\varphi(x) = \frac{1}{x + \sqrt{x^2 + \tau^2}} \quad (8)$$

where:  $\tau$  is a small increment taken as 0.05.

(2) Filling degree requirement. The layout of most public scenes requires the full utilization of space, for example, exhibitions need to be evenly placed so that all parts of the exhibition area have content. In shopping malls, the expensive space should be fully utilized to place the shelves, and so on. Eq. (9) is the energy function of the filling degree constraint  $E_u$ .

$$E_u = \sum_{V_i \in V} \varphi \left( 1 - \frac{\delta_{\min}}{\delta_{V_i}} \right) \quad (9)$$

where:  $\delta_{\min}$  is the minimum threshold of space utilization for functional area  $V_i$ .  $\delta_{V_i}$  is the actual space utilization rate. The space area occupied by a group of layout objects is determined by the sum of its footprint and its space requirement.

(3) Accessibility demand. Input contour of the functional areas are connected to each other, accessibility requirements between the connected functional areas can be reached, neighboring areas must share a wide enough channel. Equation (10) is the energy function of the accessibility constraint  $E_a$ .

$$E_a = \sum_{V_i, V_j \in V} \gamma \left( e^{\rho(d_{\min} - d_{ij})} - 1 \right) \quad (10)$$

where:  $d_{\min}$  is the minimum threshold of channel width.  $d_{ij}$  is the neighboring functional area channel width.  $\rho(\cdot)$  is the ReLU function.  $\gamma$  is a 0-1 parameter and  $\gamma = 1$  indicates that the functional areas are adjacent.

(4) Scale constraints. In order to avoid a group occupying too much space and compressing the space of other layout objects, it is necessary to control the area share of the layout object group. Eq. (11) is the energy function of the proportionality constraint  $E_p$ .

$$E_p = \sum_i \varphi \left( 1 - \frac{\rho(\mu_i - \mu_{i\max})}{\mu_{i\max}} \right) \quad (11)$$

where:  $\mu_i$  is the distance between numbered neighboring objects in the group.  $\mu_{i\max}$  is the distance parameter maximum threshold.  $\mu_{i\max} = t_{S_i} + t_{S_j} + Z$ ,  $t_{S_i}$  and  $t_{S_j}$  are the spatial requirements of individual layout objects width,  $Z$  is a constant, the smaller  $Z$  the stronger the constraint on the area share of the group.  $\rho(\cdot)$  is the ReLU function.

The energy function is weighted to form a cost function as in equation (12):

$$Er(S) = \omega_0 E_s + \omega_1 E_u + \omega_2 E_a + \omega_3 E_p \quad (12)$$

where:  $\omega_i$  is the positive weight and the value of the parameter in the experiment is  $\omega_0 = \omega_1 = \omega_2 = \omega_3 = 1.0$ .

### 2.3.2. GD-MH Algorithm

The spatial layout is optimized using a graph-driven MH layout optimization algorithm, where the input of the algorithm is the initialized layout SG and the output is the optimized layout  $SG^*$  in the following steps:

- (1) Calculate the current layout objective function  $f(SG_i)$ .
- (2) Perform one layout adjustment, if any element is out of bounds or overlapped, return to step (1). Otherwise, compute the new objective function  $f(SG_{i+1})$ .
- (3) Calculate the acceptance probability as in equation (13):

$$p = \min \left\{ 1, \frac{f(SG_{i+1})}{f(SG_i)} \right\} \quad (13)$$

Generate a random number  $rand$  in the range 0–1.

(4) If  $p < rand$ , reject this move. Otherwise, accept this move.

(5) Iteration number  $i = i + 1$ . If  $i = 1000$ , end. Otherwise, return to step (1).

Where the function equation (14):

$$f(SG) = e^{-\lambda Er(S)} \quad (14)$$

$\lambda$  is a constant taken as 0.1. In order to effectively explore the layout space, layout adjustment must consist of local adjustments that finely tune the layout and pattern changes that significantly alter the layout. The specific adjustment strategies are as follows:

(1) Expand/reduce template. The operation of expanding the template applies to the case where  $E_s$  and  $E_u$  are large. If  $E_p$  is larger, the group with the largest space occupation is shrunk, and the spacing within the group is adjusted by modifying the distance parameter of the template, and the adjustment distance is the product of a random value under a uniform distribution and  $\max\left(\frac{I-i}{I}, 0.5\right)$  where  $I$  is the maximum threshold for the number of iterations.

(2) Translation/rotation template. If there is an overlap in the space between groups or an overlap in the space between groups and wall segments, the translation or rotation operation is performed randomly. The rotation operation needs to ensure that one side of the group enclosing the box is parallel to the nearest wall segment.

(3) Lengthen/shorten wall segments. Some scenarios have a large demand for walls, and if the length of the wall in the functional area is smaller than the required length, a wall segment is generated. If  $E_a$  is larger, the wall segment is deleted to leave the channel. The formula for the required length of the wall for layout objects is  $100 \times (M + 1) + \sum_i l_i$ , where  $M$  is the number of layout objects against the wall, and  $l_i$  is the length of the occupied spreading line of a single layout object, and the unit in the formula is cm.

In the wall segment generation strategy of this paper, if there are multiple edges of the functional area contour that can be generated as a wall, the common edges of the functional areas that are not adjacent to each other in the topological order in the SG structure are prioritized. If the common edge is the only pathway between neighboring areas, a walking gap should be reserved and the location of the generated wall segment is line segment AB.

(4) Changing the pattern. If the constraints cannot be met no matter how the parameters of the pattern are adjusted, change the pattern style that does not fit. For example, change the existing ring pattern to a new chain structure that significantly changes the energy function value.

### 3. Test and Application of the GD-MH Algorithm

#### 3.1. Simulated Environmental Testing

In order to verify the effectiveness of the proposed algorithm in (A1) with the commonly used genetic algorithms:(A2) GA, (A3) PSO in the design of public space layouts, comparative experiments are conducted in a simulated environment. All feature values are normalized to the interval (0.0,1.0). The simulation experiments are based on the following assumptions: users cannot manually make feature adjustments, but they have a relatively clear overall perception of the layout design diagrams generated by the algorithm, and can accurately select images that meet their preferences.

##### 3.1.1. Comparison of Variational Operators

Provided that the final satisfactory solution is determined, i.e., the global optimal solution is known, the Euclidean distance between an individual and that solution is used as the fitness value function. A good variational operator has a considerable impact on the performance of the algorithm. In the experiments, four classical variational operators, DE1 (DE/current-to-pbest/), DE2

(DE/current-to-best/1), DE3 (DE/rand/1), and DE4 (DE/best/), were compared in order to select the most suitable operator for the internal layout model. The experiment was divided into four control groups with different difference strategies. In order to make the experimental data more accurate, the experiment was carried out in eight times, and finally the average value was chosen as the experimental data, and the comparison results of different variance operators are shown in Fig. 2.

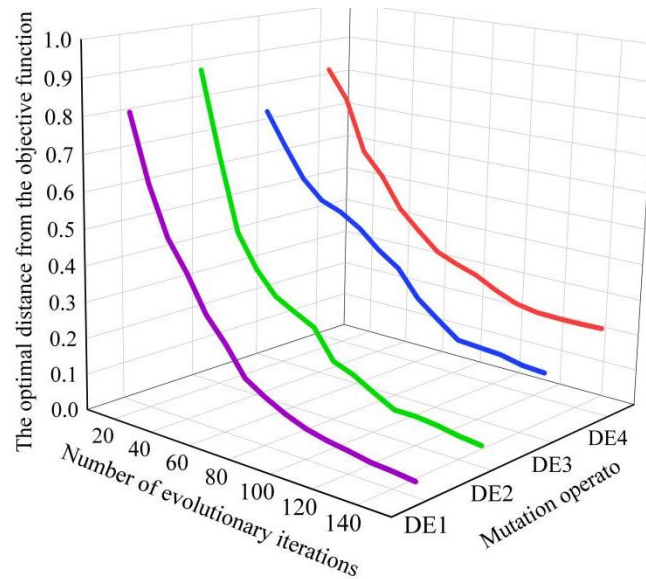


**Figure 2.** The comparison results of different mutation operators.

It can be seen that the convergence performance of the two operators DE1 and DE2 is better, and has begun to converge when the number of iterations is 80. In order to reduce the error caused by selecting the time ordering, it is more appropriate to choose DE2, which is simpler and has the same excellent performance, for the variational operator.

### 3.1.2. Simulation Tests

Taking the hypothetical target vector  $O(o_1, o_2, \dots, o_D)$  as the reference value, Fig. 3 shows the variation of the average convergence curves of the three algorithms to find the target value in 10 simulation experiments. The experimental results show that there is no significant difference between the three algorithms in the initial stage of the iteration when  $t = 20$ . In the later stage of iteration, (A2)GA converges earlier, and (A1)proposed algorithm and (A3)PSO work better. When  $t=60$ , the convergence speed and convergence accuracy (0.152) of the (A1) proposed algorithm are significantly better than the other two algorithms. In this experiment, in order to accurately verify the convergence of the algorithm, the number of iterations in the simulation experiment is set to = 150, but in a real HCI environment, the maximum number of iterations  $t \leq 50$  is usually more appropriate in order to avoid user fatigue that affects the final results.

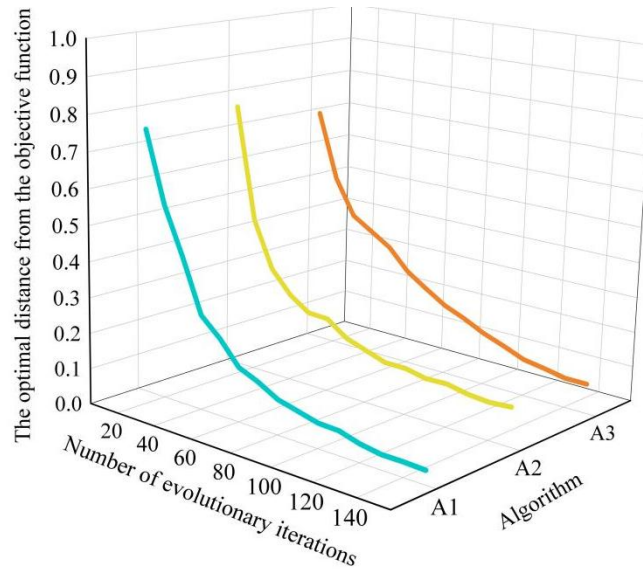
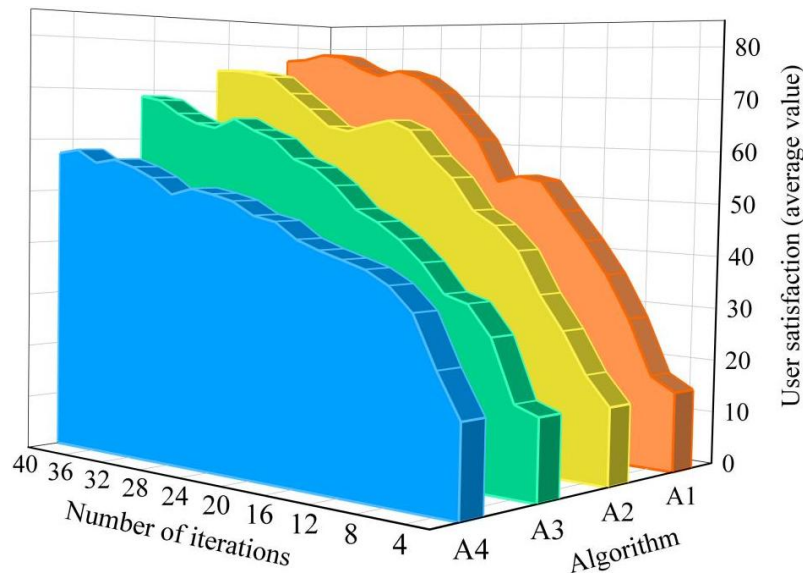


**Figure 3.** Simulation evaluation results.

### 3.1.3. Convergence Testing

In interactive algorithms, in addition to the effect of parameters on convergence, the subjective choice of the user plays a key role, and the purpose of the convergence test was to test the user satisfaction and usefulness of the system in real-world results, and to investigate the effect of the user's subjective choice on convergence during the evolutionary process. Since the characteristics of the design and art industry make a quantitative description of convergence difficult, 20 testers were selected to use the system in this experiment, setting the maximum number of iterations to 50 and investigating the testers' satisfaction with the individuals. Given that the aim of the system is to ultimately produce user-satisfied solutions, the system can be considered to have achieved its design purpose as long as a number of high-quality solutions are eventually evolved. In each iteration, testers select the individual in the group that best matches their preferences and score it on a scale from 0 to 100, then the average score given by the 20 testers in each iteration is calculated. The higher the scores for both metrics, the better the algorithm's ability to converge. When the final solution has a score of 75 or more, the system is considered to have generated a solution that the user is ultimately satisfied with. Figure 4 shows how the satisfaction level varies with the user's subjective choice and the change of the algorithm, which incorporates the algorithm: (A4)GA-PSO, with the change of satisfaction for European style in Fig. 4(a), and the change of satisfaction for Minimalist style in Fig. 4(b).



(a) "European" style

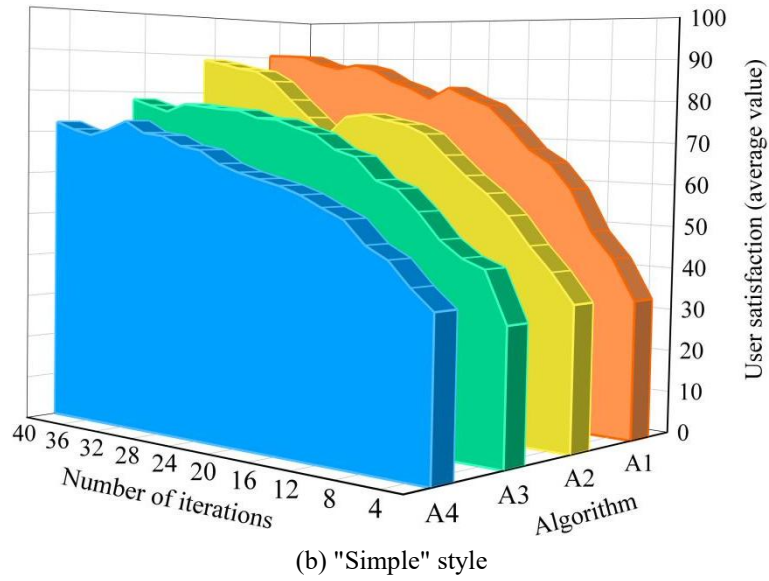


**Figure 4.** Convergence test results.

Observing Fig. 4, when the number of iterations is 0-12, none of the four algorithms has a significant effect on the results. And when  $t$  starts  $> 14$ , the algorithm proposed by (A1) starts to show better convergence ability than the other three algorithms, stemming from the fact that it is easier to jump out of the layout optimum after it falls into the layout optimum, and therefore ends up with a higher satisfaction level. And overall, the algorithm proposed by (A1) is able to obtain higher user satisfaction (15.02% to 90.56%).

### 3.1.4. Optimization Results

After 20 iterations, the proposed algorithm reaches basic convergence. Figure 5 depicts the distribution of each solution (individual) in the two-dimensional objective space during the optimization process, where the x-axis denotes the average sky visibility ratio and the y-axis denotes the façade average radiation reception, with smaller values indicating higher performance on that objective. The graph indicates all evaluated individuals up to 20 generations in green color and non-dominated solutions in yellow color. The gradual approximation of the proposed algorithm to the optimal solution can be clearly seen.

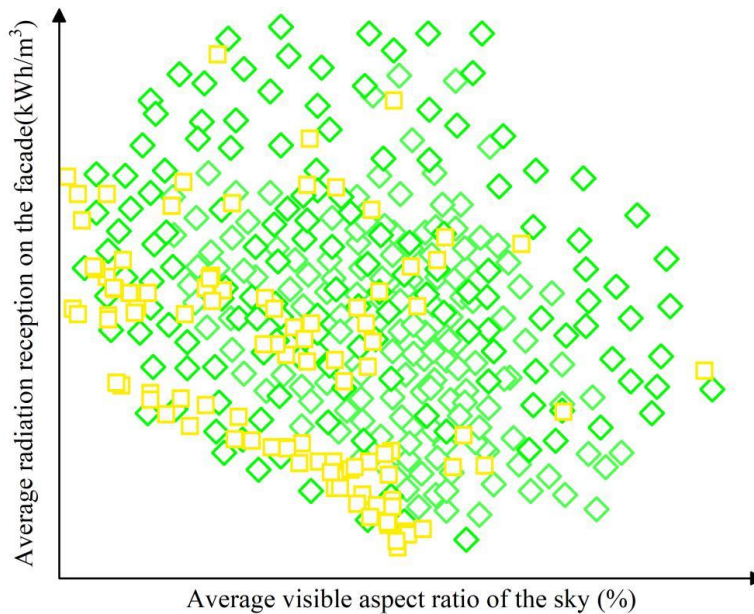


**Figure 5.** Distribution in the two-dimensional target space.

### 3.2. Evaluation and Analysis of Application Effects

#### 3.2.1. Space to Be Allocated

The space is discretized into grid cells with an area of about 5 m<sup>2</sup>, and combined with the activity definitions, the space to be allocated can be organized in Table 1. where (S1) area of a single activity cell (m<sup>2</sup>), (S2) number of points occupied by a single activity cell, (S3) number of activity areas, (S4) number of activity cells contained in a single area, and (S5) total number of grids occupied by an area.

**Table 1.** Summary of space to be allocated.

Name of the activity area	S1	S2	S3	S4	S5
Game area (small)	35	10	6	6	36
Game area (Large)			5	8	36
Gathering area (small)	25	7	6	7	34
Gathering area (large)			5	9	29
Group area (small)	15	5	6	7	22
Group Area (Middle)			8	6	28
Group Area (Large)			10	7	58
Personal area (small)	10	4	8	7	28
Personal Area (Middle)			9	6	24
Personal Area (Large)			12	6	36

#### 3.2.2. Example Analysis

In order to verify the effectiveness of the method proposed in this paper, the cited design requirement is to complete the calculation example of 30 layout object scheme design in the layout space, including 25 rectangular and 5 cylindrical layout objects. The algorithm selected GA, PSO, PPSO, CCGA, CEPPO, CEPPO\_HR a total of six methods for layout optimization effect comparison. Each algorithm is randomly calculated 80 times, and the comparison results of the seven algorithms for solving the layout design are shown in Table 2, in which the average performance indexes are: (I1) the sum of the radius of the envelope circle (mm), (I2) the unbalanced force (N), (I3) the unbalanced force even (N\*mm), (I4) the amount of interference (mm), and the best performance indexes are: (I1) the sum of the radius of the envelope circle (mm), (I2) the unbalanced force (N), (I2) the unbalanced force (N), and (I2) the unbalanced force (N\*mm). (I2) unbalanced force (N), (I3) unbalanced force couple (N\*mm).

**Table 2.** The results of solving the layout design by seven algorithms.

Algorithm	Average performance index				Best performance index		
	I1	I2	I3	I4	I1	I2	I3
GA	2921.72	11.24	2771.37	1762	2918.92	0.25	0
PSO	2915.91	15.55	7232.47	223	2833.62	0	0
CCGA	2903.92	9.5	3149.99	923	2841.18	0.07	0
CEPPO	2855.2	11.31	4007.14	339	2795.88	0	0
PPSO	2815.54	2.91	2517.15	73	2727.85	0.01	0
CEPPO_HR	2801.41	1.37	1463.31	10	2708.95	0	0
Textual	2712.94	1.06	1408.54	0	2651.24	0	0

The comparison results of the seven algorithms in Table 2 show that in the average performance index of the optimization results, none of the six comparison algorithms can make the interference reach the minimum value of 0, while this paper can make the layout scheme optimal in terms of the amount of non-interference (I3 = 0).

Table 3 gives the results of the optimized layout design scheme obtained by this paper's algorithm for solving this algorithm.

**Table 3.** Optimize the layout design scheme.

Serial number	Arrange the position and direction			
	x(mm)	y(mm)	z(mm)	$\Phi$ (rad)
1	-406	1127	-235	1.108
2	928.5	168.6	-300	1.537
3	123.5	459.4	-365	0.024
4	-249.5	992.2	180	-0.382

5	-628.8	164.4	-305	-1.493
6	513.4	220.7	195	1.349
7	-397.6	271.2	240	-1.271
8	682.8	-623.4	95	-0.619
9	181.3	-978.7	-265	-0.029
10	0.1	269.4	175	0
11	-858.8	24.6	115	0.122
12	582.8	-147.7	120	-1.014
13	-322.6	-207.9	105	0.954
14	-578.4	-756.2	-305	
15	593.7	1025.5	-350	
16	252.5	643.8	185	
17	748.7	-672.4	-335	
18	1102.1	815.7	-235	0
19	1070.9	-19.3	230	
20	-649.1	-201	165	
21	197.29	-672.7	185	
22	-588.8	695.1	65	
23	-415.9	-700.2	215	0.602
24	-539.6	677.4	165	-0.852
25	0	-212.6	215	0
26	0.5	-276.6	-185	
27	-406	1127	-235	1.108
28	928.5	168.6	-300	1.537
29	123.5	459.4	-365	0.024
30	-249.5	992.2	180	-0.382

From the results in Table 3, it can be seen that the method of this paper can make the layout design scheme of rectangular layout objects more accurate in hybrid layout solving, thus improving the performance indexes such as the sum of envelope circle radii of the layout scheme. The comparative analysis of the above examples shows that the algorithm proposed in this paper shows good computational performance in solving the layout optimization problem and obtains an excellent layout design scheme.

#### 4. Conclusion

In this paper, the information exchange between users and designers is effectively improved by using the multi-person collaborative design method, deep neural networks are utilized to assist in obtaining the spatial distribution characteristics of different functional areas in public space, and the layout scheme generation method is designed by combining the energy function with the GD-MH algorithm, so as to put forward the public space layout design method based on the GD-MH algorithm.

After simulation and comparison, it is determined that DE/current-to-best/1 is a variant of the algorithm, and the number of iterations should be less than or equal to 50. Compared with similar algorithms, the proposed algorithm starts to converge after 14 iterations, and the generated layout plan can obtain a maximum of 90.56% of user satisfaction. In the actual layout program design, this paper's algorithm layout program of non-interference amount of 0mm, reaching the optimal.

#### References

1. Amin, T. (2024). Globalization and cultural homogenization: A critical examination. *Kashf Journal of Multidisciplinary Research*, 1(03), 10-20.
2. Panjaitan, T. W., Pojani, D., & Darchen, S. (2020). Global homogenization of public space?: A comparison of "Western" and "Eastern" contexts. In *Companion to Public Space* (pp. 165-181). Routledge.
3. Lemoine-Rodríguez, R., Inostroza, L., & Zepp, H. (2020). The global homogenization of urban form. An assessment of 194 cities across time. *Landscape and Urban Planning*, 204, 103949.
4. Ding, G., Guo, J., Pueppke, S. G., Ou, M., Ou, W., & Tao, Y. (2022). Has urban form become homogenizing? Evidence from cities in China. *Ecological Indicators*, 144, 109494.
5. Chaphalkar, A. S. LACK OF WELL-DESIGNED PUBLIC SPACES AND PUBLIC ART: A CULTURAL DEFICIT OF SECOND TIER CITIES. *FOSADPAF-2023*, 39.
6. Tahseen, E., & Al-Jumaily, S. (2020). Mechanisms for reviving the intangible cultural heritage to revitalize urban spaces. *International Journal of Environment, Engineering and Education*, 2(3), 31-42.

7. Schmidt, S., & Németh, J. (2010). Space, place and the city: Emerging research on public space design and planning. *Journal of Urban Design*, 15(4), 453-457.
8. Song, L. (2024). The street space planning and design of artificial intelligence-assisted deep learning neural network in the Internet of Things. *Heliyon*, 10(15).
9. Zheng, X. (2025). Research on artificial intelligence-assisted green space layout in environmental design for smart cities. *International Journal for Housing Science & Its Applications*, 46(1).
10. Yin, X., Li, J., Kadry, S. N., & Sanz-Prieto, I. (2021). Artificial intelligence assisted intelligent planning framework for environmental restoration of terrestrial ecosystems. *Environmental Impact Assessment Review*, 86, 106493.
11. Kang, Y. (2025). An AI-driven urban landscape planning decision support system using PSO and knowledge graphs. *GeoJournal*, 90(3), 1-18.
12. ZHOU, H., & XIANG, S. (2024). Applicability Evaluation and Reflection on Artificial Intelligence-based "Image to Image" Generation of Landscape Architecture Masterplans. *Landscape Architecture Frontiers*, 12(2), 58-67.
13. Guridi, J. A., Cheyre, C., Goula, M., Santo, D., Humphreys, L., Souras, A., & Shankar, A. (2025). Image generative ai to design public spaces: a reflection of how ai could improve co-design of public parks. *Digital Government: Research and Practice*, 6(1), 1-14.
14. Li, H., Wu, Q., Xing, B., & Wang, W. (2023). Exploration of the intelligent-auxiliary design of architectural space using artificial intelligence model. *Plos one*, 18(3), e0282158.
15. Chen, T. Y., Huang, C. S., & Sung, W. P. (2025). Improving summer outdoor comfort in metropolitan park: a data-driven approach using AI, experimental and design analysis. *Journal of Measurements in Engineering*.
16. Quan, S. J., Park, J., Economou, A., & Lee, S. (2019). Artificial intelligence-aided design: Smart design for sustainable city development. *Environment and Planning B: Urban Analytics and City Science*, 46(8), 1581-1599.